World Journal of Engineering Research and Technology

WJERT

FINITE ELEMENT MODEL OF CORRODED-DAMAGED REINFORCED CONCRETE PILE USING ABAQUS

Cecielle N. Dacuan[1]*, Virgilio Y. Abellana PhD[1] and Hana Astrid Canseco-Tuñacao PhD[1]

Engineering Graduate Program, School of Engineering, University of San Carlos, Philippines.

*Corresponding Author
Cecielle N. Dacuan
Engineering Graduate
Program, School of
Engineering, University of
San Carlos, Philippines.

ABSTRACT

This study presents a finite element model of reinforced concrete square pile structures using the ABAQUS program. Concrete damaged plasticity (CDP) was used to model the behavior of both corroded and uncorroded reinforced concrete piles. The CDP parameters were calibrated and compared with the control model to validate the

accuracy of the results of the parametric study. A numerical parametric analysis was performed to investigate critical parameters such as cracking of the concrete, steel cross-sectional area reduction, and degradation of the bonding strength of concrete materials and steel reinforcement rebars. The results verify that the loss of strength of the steel rebars and concrete has a significant influence on the residual life and serviceability of reinforced concrete pile columns. It was verified that the selected nonlinear finite element analysis FEA simulated the behavior of corrosion-deteriorated pile columns accurately, and the numerical results established good correlations with the experimental results. Constructing a finite element analysis (FEA) model to simulate the effects of corrosion on reinforced concrete piles using ABAQUS is in good agreement with the experimental results and the deterioration of actual reinforced concrete piles. The stresses exerted by the corrosion products lead to the initiation of corrosion beneath the concrete surface. The loss of bonds between concrete and steel causes sudden failure, and the elements behave as unreinforced columns. The crack pattern depends on the bond strength. The spalling of concrete at the upper part requires more anchor reinforcements to avoid early deterioration due to corrosion.

If the pile has a sufficient embedded length and the steel reinforcement is well anchored at their ends, a reduction in bond strength does not affect its serviceability and residual life.

KEYWORDS: ABAQUS software, Corrosion, Reinforced Concrete Pile Columns, Concrete Damage Plasticity, concrete failure, Finite element analysis.

I. INTRODUCTION

The environmental conditions in which the structural elements are located and exposed have a significant influence on the deterioration of structures.[7,19] Steel reinforcement corrosion is the most frequent deterioration caused by chloride attack and carbonation of concrete itself, particularly in structures located in an aggressive marine environment.[9,10] It is considered to be the most serious durability concern for reinforced concrete structures, especially in coastal regions.[3,4] The loss of life and property owing to corrosion deterioration has led researchers to work on this natural phenomenon.[22] Thus, several researchers have attempted to study the corrosion of steel reinforcements of structural elements.[16]

The corrosion behavior of structures exposed to harsh environments, such as reinforced concrete piles, is quite different compared to other exposure conditions.[16] The strength of reinforced concrete piles should be investigated while they are exposed to corrosion to determine the loss of strength and serviceability. The adequacy of the corroded reinforced concrete pile to withstand the applied loads is important to avoid unnecessary and expensive costs of rehabilitation and repair from an over-conservative load rating of the deteriorated structures.[19] Fig. 1 shows a photograph of the corroded reinforced concrete piles.

Corroded reinforced concrete piles experience severe deterioration, which eventually affects the integrity and load-carrying capacity of the structures.[4] The major detrimental effects of corrosion include cracking, reduction of the steel reinforcement area and its mechanical strength, and degradation of the bond strength between steel and concrete.[3,4,16] According to Al-Sakkaf and Ahmdi, the complete loss of bond between the steel reinforcement and concrete is the most critical damage induced by corrosion. Bond strength deterioration leads to sudden failure, and the structures behave as unreinforced structural elements.[3,4] It weakens its static bearing capacity and increases its brittleness. Thus, it is important to study the bond degradation characteristics of the corroded structural members.[11]

Figure 1: Photo of Corroded Reinforced Concrete Pile.

The corrosion of reinforced concrete structures has been investigated by several researchers from different viewpoints.[16] However, corrosion deterioration can be explained clearly in three-dimensional 3D models that describe the most detrimental deterioration, de-bonding of concrete, and steel reinforcement.[22] Finite element analysis, according to Du (2016), illustrates the behavior of structural elements in experimental tests.[9] Modeling the bond degradation of steel rebars and concrete induced by corrosion is beneficial for predicting the residual life and capacity of corroded reinforced concrete members.[3] In addition, it was used to simulate the influence of various corrosion indices on the structural elements. However, several problems arise when creating an accurate FE model of the existing structure. Errors include parameters such as structural damage, material uncertainties, and geometrical properties. Thus, the finite element model should be calibrated in a realistic manner according to the experimental results to obtain a suitable finite element model.[22]

Khalid (2018) evaluated the load-carrying capacity of deteriorated columns by considering concrete cover spalling at different locations in the columns. A numerical analysis was performed by developing a 3D finite element model in ABAQUS. The results verified that increasing the required steel reinforcement area enhanced the performance of the deteriorated columns. Finite element analysis with ABAQUS was in good agreement with the experimental results, and it was possible to simulate the column behavior using the FE model.[19] Al-Sakkaf thoroughly investigated the FE modeling of corroded RC beams and uncorroded beams as control structural elements. A finite element of the 3D model using ABAQUS was developed, and the three major effects of corrosion-induced damage were

considered, including the loss of bond strength, concrete cracking, and reduction of the steel reinforcement area. Furthermore, according to Al-Sakkaf, a mechanical model based on traction-separation behavior, also known as surface-based cohesive behavior, was found to be accurate in modeling bond deterioration in a 3D model.[4] Du et al. investigated the deterioration of the bond strength of steel reinforcements and concrete owing to corrosion. The thickness of the concrete was represented by a thick-wall cylinder, and the evaluation of its bond strength capacity was verified against published bonding test results. The results illustrate that the reduction in bond strength between steel and concrete due to corrosion is the main cause of flexural degradation, and the most significant deteriorated performance is noted in the specimen with only bond deterioration taken into account.[9] Al-Osta et al. (2018) modeled RC beams via 3D nonlinear FE analysis in abaqus, both for corroded and uncorroded beams that exhibited different failure modes. Contact friction, which is a function of the degree of corrosion, was used to model the interface between the concrete and steel. A suitable reduction of their non-corroded properties or the removal of spalled concrete were used to model the damage to concrete and steel elements due to corrosion.[3] Hansen and Saoma modeled a simulation of the reinforced concrete deterioration of a concrete bridge deck. Nonlinear fracture analysis was used to investigate the concrete fractures caused by corrosion in the steel reinforcing bars. The results of the study indicate that the propagation of cracks in both the horizontal and vertical directions is due to tensile effects, and the propagation of cracks in the diagonal direction is due to shear effects. In addition, the extent of cracks depends on the stirrup spacing and concrete cover.[13] Jayasinghe et al. (2018) performed experiments to illustrate the propagation of corrosion in embedded steel reinforcements, where one is directly exposed to aggressive agents. A numerical model was developed to illustrate incremental corrosion propagation. The damage due to concrete corrosion was enhanced owing to the direct exposure of the steel reinforcement. The results of the study verified that different aeration corrosions play a significant role under these circumstances. In addition, the porosity of concrete influences the corrosion of embedded steel reinforcements.[16]

Very few studies have been conducted on corroded reinforced concrete structures, especially considering the bond loss in modeling. There is a lack of 3D FEM for corroded reinforced concrete piles, which would enable researchers to study the behavior of such structures.
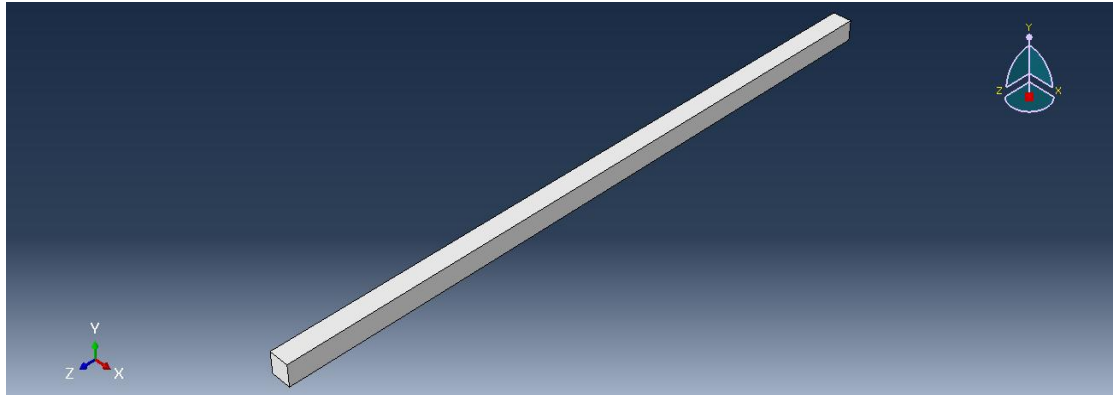
The main objective of this study was to simulate the behavior and performance of corroded reinforced concrete piles using a 3D finite element model. The 3D model predicts the behavior and load-carrying capacity of corroded reinforced concrete piles with reasonable accuracy. A 3D model was developed using the ABAQUS finite element model to simulate corroded reinforced concrete piles, considering all corrosion-indulged deteriorations, such as bond strength reduction of steel and concrete, cracking and spalling of concrete cover, and reduction in the steel area and degradation in the mechanical properties. To provide a reference for the maintenance and performance evaluation of reinforced concrete pile columns, a simulation of corrosion-induced degradation using ABAQUS was performed. Therefore, the behavior of the corroded reinforced concrete pile was determined by numerical analysis using detailed FE 3D modeling.
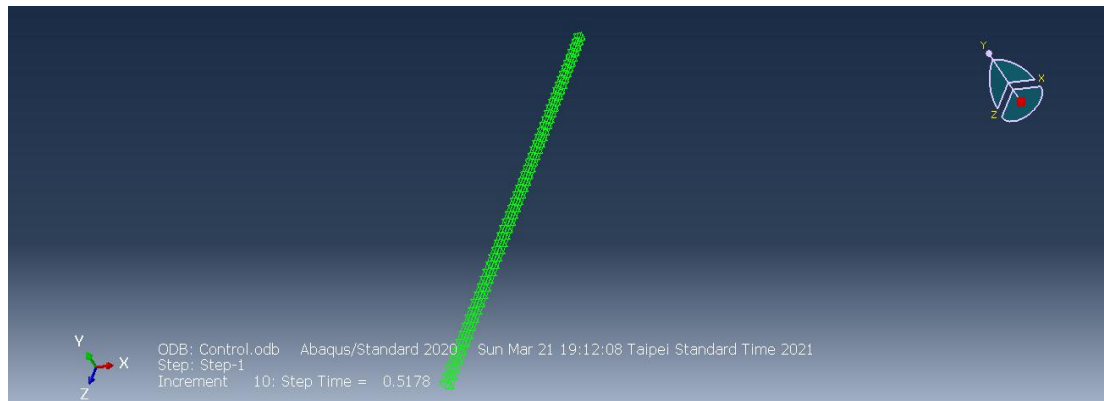
II. Numerical simulations

2.1 Finite Element Modelling of Uncorroded Structure

The nonlinear finite element package ABAQUS was used in the numerical finite element method in this study. It was used to analyze the failure capacity of corroded damaged reinforced concrete piles. The finite element modeling FEM method of ABAQUS is the most practical and widely used modeling software. It is specifically used to estimate the capacity of reinforced concrete structures. It has been significantly developed since 1970 and is widely used in the analysis of the behavior of reinforced concrete structures.[4]

In modeling the structural elements, the geometrical and material parameters and their boundary conditions were analyzed in detail. Reinforced concrete materials were modeled as homogeneous 3-dimensional solid sections. A schematic of the FE model is presented in Fig. 2. Solid elements (C3D8R) were used for the concrete and longitudinal steel rebars, and truss elements (T3D2) were used for the stirrup bars. A hard contact was applied in the normal direction. The embedded element technique was used to simulate the interaction between rebar and concrete. A concrete-damaged plasticity model was used for the concrete.
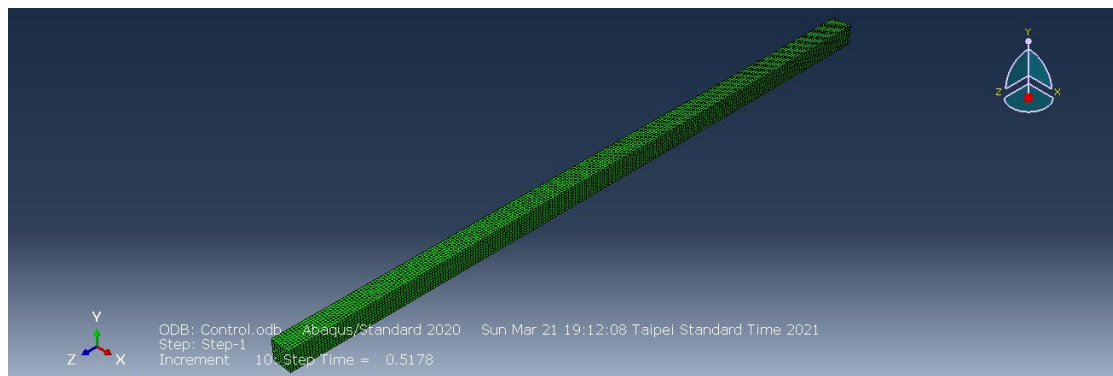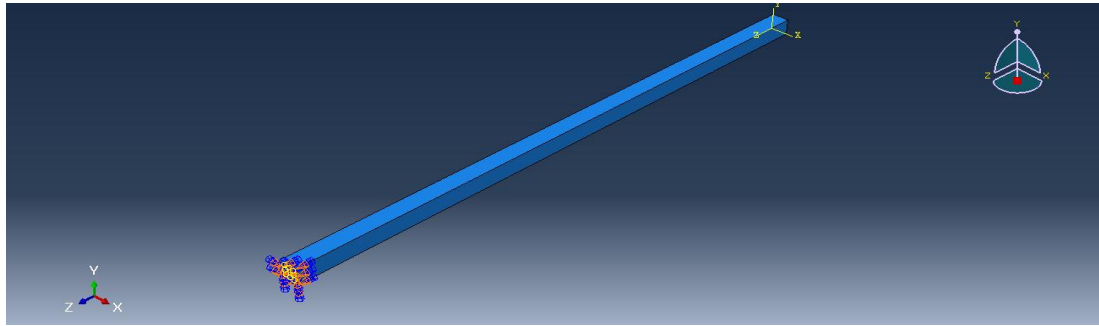
a)

b)

c)

d)

e)

Figure 2. A schematic view of the FE model: a) Geometry, b) Steel Mesh, c) Embedded Region Contraints, d) Finite Element Meshing, and e) Boundary Conditions.

2.1.1 Model Geometry, Boundary Conditions, and Loadings

The embedded region constraint was used to present the bonding of the steel reinforcement, stirrups, and concrete of the uncorroded structures. This limits the nodes based on the degrees of freedom of the host region elements. Reinforced concrete piles were fixed at the top and bottom supports, and axial loading was applied at the top end. A uniform concentric loading of 3KN and a displacement of 200 mm were applied to the free end of the reinforced concrete piles.

2.1.2 Uncorroded Reinforced Concrete Pile Column Model

The section of the reinforced concrete pile column was 300 mm × 300 mm, and the total length of the column was 10meters. The main vertical reinforcement was 8−16 mm in diameter. The stirrup was a rebar with a diameter of 10 mm and a spacing of 190 mm at the center. The properties of the reinforced concrete pile column model are listed in Table 1. Table 2 lists the geometric and material characteristics of the structural column model. Fig. 2 shows a typical reinforced uncorroded concrete pile column. ACI code was used to calculate the elastic modulus (E_c) of the concrete.

$$E_c = 4700 \sqrt{f`_c} \tag{1}$$

Table 1: Concrete Properties.

Parameter	Value
Concrete density (ton/mm^3)	2.40x 10^{-9}
Poisson`s ratio, v	0.20
Young`s Modulus, Ec (N/mm^2)	26587
Concrete cover thickness (mm)	50
Initial and maximum increment size	0.01
Minimum increment size	10^{-10}

Table 2: Geometric and Material Characteristics of column specimens.

Structure Label	Reinforcement Type	Compressive Strength of Concrete (MPa)	Main Reinforcement		Concrete Cover thickness (mm)	Transverse Reinforcement		Test Eccentricity (mm)
			Rebars	Reinforcement Ratio(%)		Diameter of rebars (mm)	Spacing (mm)	
Reinforced Concrete Pile	Steel	32	8-16mm	1.63	50	10	190	45

2.1.3 CDP Parameters

Concrete is a brittle material, and its behavior is complex. It exhibits different behaviors in terms of compression and tension.[19] The nonlinear stress–strain relation of concrete under imposing stress conditions and the strain hardening or softening behavior of concrete are complicated, making it difficult to determine the damage in concrete.[4]

The three (3) cracking models used to simulate the damage in the concrete elements using ABAQUS are the smeared crack concrete model, brittle cracking model, and concrete damaged plasticity model. In the CPD model, tensile cracking and compressive crushing are the two main failure mechanisms of concrete materials.[4,12,19,20] The concrete damaged plasticity CDP was used to model the behavior of reinforced concrete structures and the failure mechanisms of concrete elements.[12]

The hardening and softening variables were used to determine the cracking and crushing trends, the development of the yield surface, and the loss of the elastic stiffness of the concrete. Tension and compression are two parameters that affect the material stiffness [15, 20]. Plastic strains in compression ($\varepsilon_c^{pl,h}$) and plastic strains in tension ($\varepsilon_t^{pl,h}$) are the two hardening variables that characterize the damage states under compression and tension, respectively.[4] A typical stress-strain curve for concrete is shown in Figure 3.
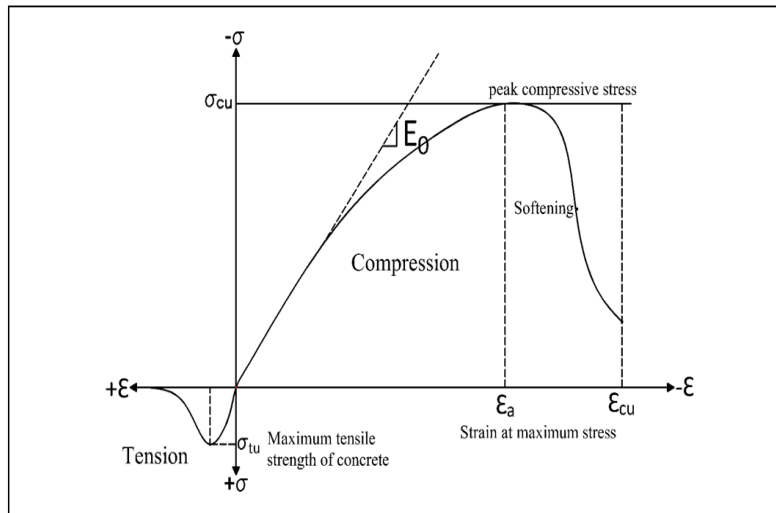
Figure 3: Typical Concrete Compressive and Tensile Stress-Strain Curve[15] (unclear) (unclear).

CDP is commonly used to model the nonlinear behavior of reinforced concrete structures. CDP deals with plastic, compressive, and tensile behavior, as well as the confinement and damage mechanism of concrete. The use of the CDP approach in finite element modeling can result in sufficient numerical results when compared to experimental tests.[19] The CDP model was developed by Lubliner et al. in 1989 and further revised by Lee and Fenves in 1998. The theory of compressive plasticity, isotropic tensile strength, and damaged elasticity was used to represent the inelastic behavior of concrete.[4]

In this study, the concrete behavior was modeled using the CDP finite element method. It consists of the plastic, compressive, and tensile behaviors of the concrete.

2.1.3.1 Plastic Behavior of Concrete

The CDP parameters include Poisson's ratio, elastic modulus, compressive and tensile behavior, and five plastic damage parameters. Five plastic damage parameters include the dilation angle (ψ), flow potential eccentricity (ε), ratio of initial equibiaxial compressive yield stress to initial compressive yield stress ($f_{bo}/f_{co)}$, ratio of the second stress invariant on the tensile meridian (k_c), and viscosity parameter (μ).[4]

The dilation angle (ψ) is the volume strain over the shear strain, which affects the ductility of the concrete. Its value usually ranges from 20^0 to 40^0, and an increase in its value also increases the flexibility of the system. The two parameters that affect the internal dilation angle are the confined pressure and plastic strain. It has an inverse relationship, and

increasing both parameters decrease the internal dilation angle.[4] A higher dilation angle value results in positive volumetric strains, which causes an increase in the bearing capacity in the compression zone of the structural elements.[20] The dilation angle was 31° for uniaxial tensile and compressive failures.[9]

The default flow potential eccentricity (ε) was 0.10. The flow potential eccentricity also increases by increasing the curvature value.[4] The ratio of the initial equibiaxial compressive yield stress to the initial uniaxial compressive yield stress was represented by f_{b0}/f_{co}, and its default value was 1.16. Abaqus software uses a null default viscosity parameter such that viscoplastic regularization does not occur.[4] Higher values of the viscosity parameter indicate the spread of damage to many finite elements through the diffuse pattern of cracks and crack propagation. A value of 0.00025–0.001 is in good agreement with the experimental results.[20]

2.1.3.2 Concrete Behavior in Compression

Uniaxial compressive behavior can be characterized by experimental tests or existing constitutive models. Fig. 4 shows a schematic illustration of the stress-strain relation for uniaxial compression. The linear elastic behavior can be taken up to $0.40f_{cm}$.
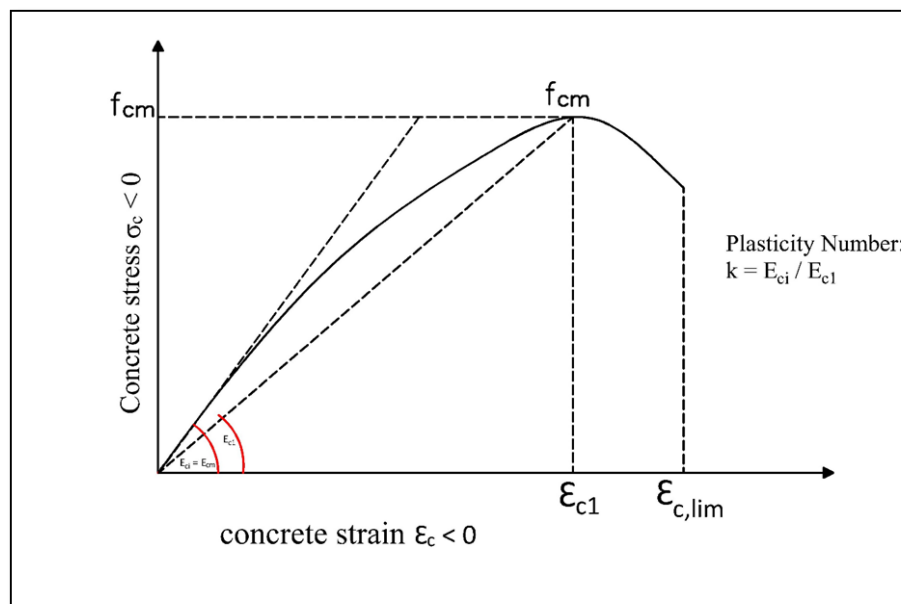

Figure 4: Schematic illustration of the stress-strain relation for uniaxial compression.[3] (unclear).

The following equation was proposed by Majewski based on the experimental results in determining the strain ε_{c1} and ultimate strain ε_{cu1}, at the average compressive strength of concrete.

$$\varepsilon_{c1} = 0.0014[2 - e^{-0.024 fcm} - e^{-0.140 fcm}] \quad (2)$$

$$\varepsilon_{cu1} = 0.004 - 0.0011[1 - e^{-0.0215 fcm}] \quad (3)$$

The plastic hardening strain in compression $\varepsilon_c^{pl,h}$ was used to determine the correlation between the compressive strength and damaged parameters of concrete. The following equations illustrate the derivation of the uniaxial compressive behavior of concrete. To determine the hardening and softening behavior of concrete under compression, Equation 4 is used.[4]

$$\sigma_c = (1 - d_c)E_0(\varepsilon_c - \varepsilon_c^{pl,h}) \quad (4)$$

$$\begin{cases} \varepsilon_c^{in,h} = \varepsilon_c - \dfrac{\sigma_c}{E_0} \\ \varepsilon_c^{pl,h} = \varepsilon_c - \dfrac{\sigma_c}{E_0}\left(\dfrac{1}{1-d_c}\right) \end{cases} \quad (5)$$

$$\varepsilon_c^{pl,h} = \varepsilon_c^{in,h} - \dfrac{d_c}{(1-d_c)}\dfrac{\sigma_c}{E_0} \quad (6)$$

$$\sigma_c = \sigma_{cu}\left[2\left(\dfrac{\varepsilon_c}{\varepsilon_c'}\right) - \left(\dfrac{\varepsilon_c}{\varepsilon_c'}\right)^2\right] \quad (7)$$

Where

σ_c = nominal compressive stress

ε_c = nominal compressive strain

σ_{cu} = ultimate compressive strength

ε_c' = ultimate compressive strain

        (0.002)

To model the stress-strain relationship of concrete materials, Eq. 8 is used:

$$\sigma_c = f_{cm}\dfrac{k\eta - \eta^2}{1 + (k-2)\eta} \quad (8)$$

Where

$$k = 1.05\, E_{cm}\dfrac{\varepsilon_{cl}}{f_{cm}} \quad (9)$$

$$\eta = \dfrac{\varepsilon_c}{\varepsilon_{cl}} \quad (10)$$

2.1.3.3 Concrete Behavior in tension

A stress–strain relationship was used to simulate the tensile behavior of the concrete. This is to consider the interaction of steel reinforcement with concrete strain softening and tension stiffening.

The behavior of concrete in tension is linearly elastic until cracks are initiated. After concrete cracking, softening behavior occurs, and the post-tension behavior for direct straining is modeled with tension stiffening.[4,19] This behavior was characterized by a stress-strain response curve, as shown in Figure 5.
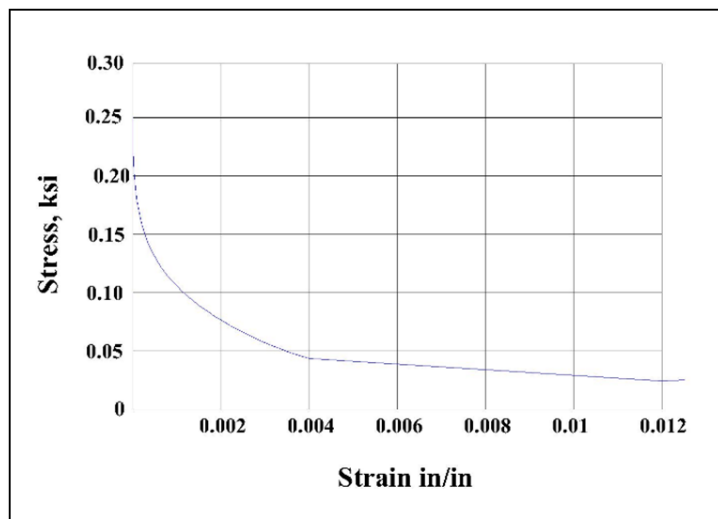

Figure 5: Tension Response Curve of Concrete.[15]

Equation 11 was proposed by Wang et al. and Genikomsou and Polak to calculate the ultimate tensile strength of concrete:

$$f_t^{`} = 0.33\sqrt{f_c^{`}} \text{ (MPa)} \qquad (11)$$

In concrete damage plasticity models, the plastic hardening strain in tension $\varepsilon_t^{pl,h}$ was derived as follows.[3]

$$\sigma_t = (1 - d_t)E_0(\varepsilon_t - \varepsilon_t^{pl,h}) \qquad (12)$$

$$\begin{cases} \varepsilon_t^{ck,h} = \varepsilon_t - \dfrac{\sigma_t}{E_0} \\ \varepsilon_t^{pl,h} = \varepsilon_t - \dfrac{\sigma_t}{E_0}\left(\dfrac{1}{1-d_t}\right) \end{cases} \qquad (13)$$

$$\varepsilon_t^{pl,h} = \varepsilon_t^{in,h} - \dfrac{d_t}{(1-d_t)}\dfrac{\sigma_t}{E_0} \qquad (14)$$

By increasing the hardening cracking strain $\varepsilon_t^{ck,h}$, the tension damage continued to increase. The elasto-plastic behavior with hardening was considered as the modulus of elasticity equal to $E_s=200,000$ N/mm^2 and Poisson's ratio equal to $v=0.30$.[3] A value of 1 for a tensile damage variable indicates a total loss of capacity, and a value of 0 indicates the fresh state of the concrete specimen.[20]

A linear stress-strain relationship up to 0.50 ultimate stress is used in compression, the stress in the descending part was calculated using the numerical model by Hsu amd Hsu (1994), Wahalathantri, et al., (2011) given by:

$$\sigma_c = \left[\frac{\beta\left(\varepsilon_c/\varepsilon_o\right)}{\beta-1+\left(\varepsilon_c/\varepsilon_o\right)^\beta} \right] \sigma_{cu} \quad , \quad ksi \qquad (15)$$

$$\beta = \frac{1}{1-[\sigma_{cu}/\varepsilon_o E_o]} \qquad (16)$$

$\varepsilon_o = 8.9\text{x }10^{-5}\sigma_{cu} + 2.114\text{x}10^{-3}$ (17)

$E_o = 1.2431\text{x}102\ \sigma_{cu} + 3.28312 \text{ x } 10^3$

, ksi   (18)

ε_o , E_o are the maximum strain and initial tangential modulus of elasticity, respectively. $E_{d\ strain}$ is iteratively calculated using eq. 15 when $\sigma_c = 0.80\ \sigma_{cu}$
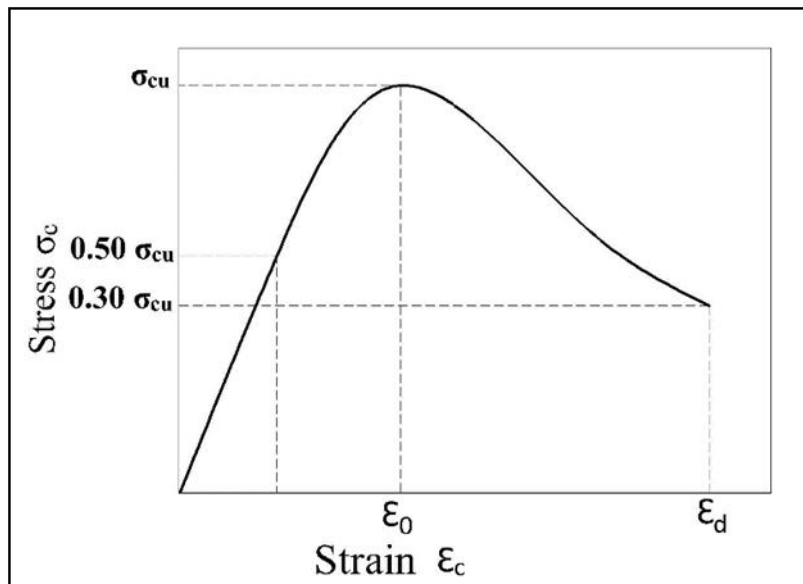

Figure 6: Compressive Stress-Strain Relationship for ABAQUS.[20]

The brittle behavior of concrete is characterized by a stress-displacement response. The fracture energy G_f associated with the failure tensile stress f_t is specified directly in the material property. Concrete assumes a linear loss of strength with crack propagation, as shown in Figure 7.

Figure 7: Post-Failure Stress-Fracture Energy Curve.[22]

The fracture energy G_f has a typical range of values from 40 N/m for concrete with a compressive strength of 20 MPa to 120 N/m for high-strength concrete with a compressive strength of approximately 40 MPa.[1]

$$f_r = 0.62\sqrt{f'c} \qquad (19)$$

The fracture energy designated as G_f is computed as:

$$G_f = 73\,(f_t)^{0.18} \qquad (20)$$

Figure 8: Stress vs. crack widths (uniaxial tension).[20]

2.1.2.3 Compression and tension damage parameters

To determine the compression and tension damage parameters, the following equations were used.[3]

$$d_c = 1 - \frac{\sigma_c E^{-1}}{\varepsilon_c^{pl}\left(\frac{1}{b_c}-1\right)+\sigma_c E^{-1}} \qquad (21)$$

$$d_t = 1 - \frac{\sigma_t E^{-1}}{\varepsilon_t^{pl}\left(\frac{1}{b_t}-1\right)+\sigma_t E^{-1}} \qquad (22)$$
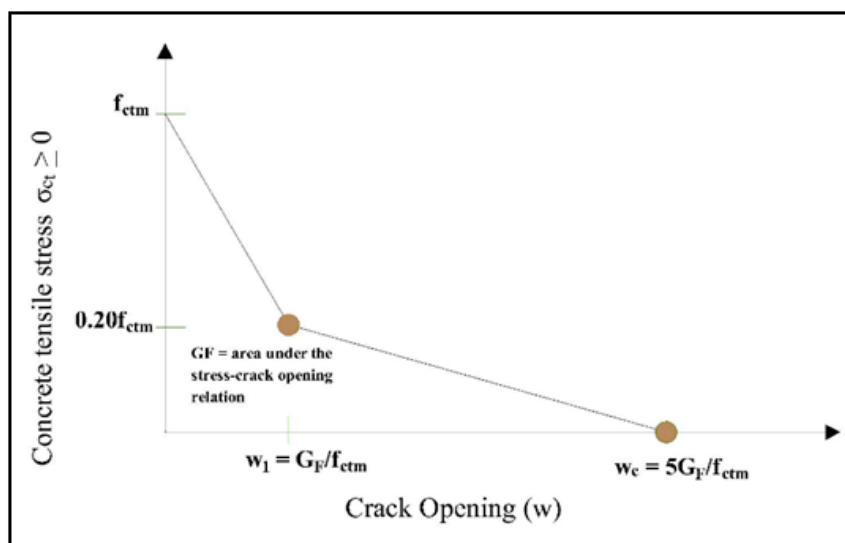
Where the values of $d_c = 0.40$, and $d_t = 0.80$.

2.1.2.5 Modelling of Steel Reinforcement

A classical metal-perfectly plastic model was used to simulate steel reinforcement. Embedded elements were used, where concrete was the host element. The displacement of the reinforcement elements is compatible with the displacement of the surrounding concrete element. The advantage of this model is that the reinforcement can be represented regardless of its location or distribution. A perfect bond between concrete and steel can be assumed in this model because the degrees of freedom for the reinforcement nodes are eliminated to be the same as those of the concrete nodes.[19]

The inputs for the steel model include the elastic modulus, Poisson's ratio, and yield stress with values of 200,000 MPa, 0.30, and 280 MPa, respectively. Table 3 shows a summary of the concrete properties used in the finite element modeling of the uncorroded reinforced concrete piles.

Table 3: Summary of Concrete Properties used in FE Modelling of RC Uncorroded Piles.

Elasticity		Plasticity Parameters				
Modulus of Elasticity	**Poisson's Ratio**	**Dilation Angle**	**Eccentricity**	**F_{bo}/f_{co}**	**K**	**Viscosity Parameter**
30 GPa	0.20	36 deg	0.10	1.16	0.67	0
Compressive Behavior			**Compression Damage**			
Yield Stress (MPa)	**Inelastic Strain**		**Damage Parameter C**		**Inelastic Strain**	
20.40	0		0		0	
25.60	2.607E-05		0		2.66667E-05	
30	0.00008		0		0.00008	
33.60	0.00016		0		0.00016	
36.40	0.000266667		0		0.000266667	
38.40	0.00004		0		0.00004	

39.60	0.00056	0	0.00056
40	0.000746667	0	0.000746667
39.60	0.00096	0.01	0.00096
38.40	0.0012	0.04	0.0012
36.40	0.001466667	0.09	0.001466667
33.60	0.00176	0.16	0.00176
30.00	0.00208	0.25	0.00208
25.60	0.002426667	0.36	0.002426667
20.40	0.0028	0.49	0.0028
14.40	0.0032	0.64	0.0032
7.60	0.0003626667	0.81	0.003626667
Tensile Behavior		**Tension Damage**	
Yield Stress (MPa)	**Cracking Strain**	**Damage Parameter T**	**Cracking Strain**
4	0	0	0
0.04	0.001333333	0.99	0.001333333

2.1.2.6 Boundary Conditions

The boundary condition represents the structural support values of the displacement and rotation variables at the appropriate nodes. For the top end of the column, the boundary condition represents the load with its specific eccentricity, which was applied in the form of displacement similar to that in the experiments, so it was restrained in the x and y directions, and the load was applied in the z-direction; for the bottom end, the boundary condition represents the support that was restrained in the x,y, and z directions.

2.1.2.7 Mesh and Convergence

All the modeled parts, including the concrete, reinforcement bars, and stirrups, were merged into the assembly module. Mesh convergence was performed on the combined part to give more accurate results with reasonable time for analysis, and a mesh size of 0.40 inches was used for analysis, as shown in Fig. 8.

The FE model is a 3D dimensional solid element, C3D8R. It is an 8-noded linear brick element type, both for concrete and main-vertical reinforcement rebars, and two-node elements (T3D2). T3D2 is a 2-noded linear 3D truss element type for stirrups.[4] All parts were modeled as 3D-solid elements using 8 node brick element C3D8 with degrees of freedom in the x,y, and z directions at each node to predict the failure load, deformation, and stresses and strains in both concrete and steel.

After meshing, the brick elements had a face dimension of 300-mm. The model of the piles was fixed at one end and the roller support at the upper end.

2.1.2   Bond Modeling of Uncorroded Reinforced Concrete Piles

The control model was simulated by calibrating the dilation angle, stress ratio, shape factor, plastic potential eccentricity, and viscosity parameter of the concrete damaged plasticity CDP model, different element types, and mesh sizes to achieve better results than previous experimental results. Fig. 9 shows the load-deflection curves for the uncorroded column piles.
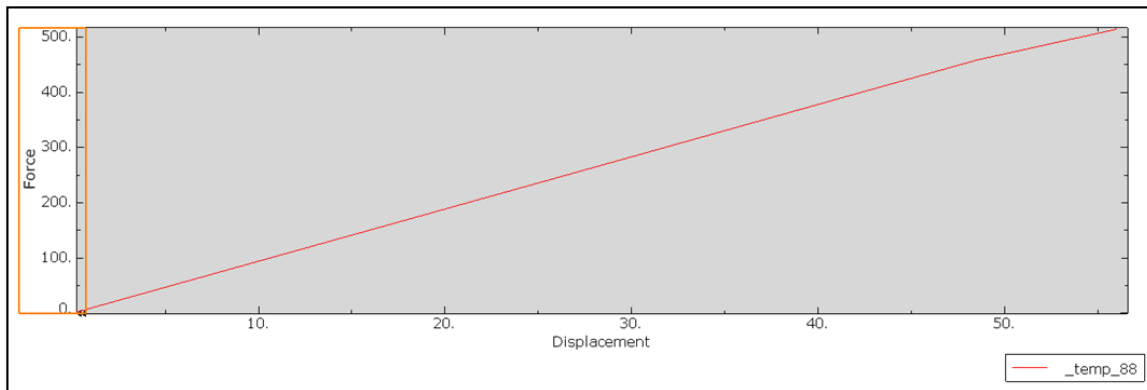

Figure 9: Load-Deflection curve for Perfect Bond Method for Uncorroded Column-Pile (Perfect Bond).

2.2 Finite Element Modelling Of Corroded Structure

In modeling non-corroded columns, a perfect bond assumption was made.[3] However, in modeling the finite element of corroded structures, the properties of uncorroded reinforced concrete pile materials were modified to reflect the damage caused by corrosion.[4] Thus, owing to non-uniform corrosion in the pitting deterioration of steel rebars, it is quite difficult to model corroded reinforced concrete piles.[4] The following were considered in the FE analysis of the corroded reinforced concrete piles, cracking of the concrete cover, steel area reduction, and reduction of bond-slip properties.

2.2.1   Reduction in Strenght of Concrete due to Cracking

Corrosion products exert pressure on the surfaces of the steel and concrete. A further volume expansion produces splitting stresses on the concrete, eventually leading to concrete cover cracking.[4] In general, the cracking of concrete surfaces affects the behavior of reinforced concrete structures.

Al-Sakkaf and Ahmed used an equation to determine the reduced compressive strength of cracked concrete structures due to corrosion.

$$f_{cc,cracked} = \frac{f_c'}{1 + k\frac{\varepsilon_1}{\varepsilon_0}} \qquad (23)$$

Where

fc' = compressive strength

K = coefficient of bar diameter and roughness,

(K = 0.10, for ribbed bars with moderate diameters)

ε_o = strain value at the highest compressive strength fc',

ε_1 = average tensile strain in the cracked concrete normal to the direction of the applied compression

$$\varepsilon_1 = \frac{b_f - b_0}{b_0} \qquad (24)$$

Where:

b_o = is the undamaged member section width

b_f = is the member width increased by corrosion cracking

$$(b_f - b_o) = n_{bar}w_{cr} \qquad (25)$$

$$\sum w_{cr} = 2\pi \left(\frac{vr}{s} - 1\right) P_r T \qquad (26)$$

2.2.2 Reduction in Steel Bar Properties

The corrosion of deformed steel reinforcements causes a reduction in the cross-sectional area. Structures exposed to a marine environment experience pitting corrosion deterioration in the reinforcement steel. The steel cross-sectional area reduction during pitting corrosion is not uniform. However, the reduction in the steel cross-sectional area is dependent on the amount of mass loss.[4] Al-Sakkaf and Ahmed used Equation 27 to determine the residual area of corroded deformed steel reinforcement.

$$A_s = (1 - 0.01x_p)A_{so} \qquad (27)$$

Where:

A_s =   Residual area

A_{so} =   Original area of the rebar

before corrosion

x_p =   Amount of mass loss

Corrosion rates have a non-linear relationship with the residual yield and ultimate forces of the steel reinforcement. With an increase in the corrosion level and reduction in the steel reinforcement area, the residual yield (F_{yc}) and ultimate forces (F_{uc}) decreased more rapidly.

Therefore, in addition to the decrease in the steel cross-sectional area, there was a reduction in the yield stress fy. Furthermore, according to Al-Sakkaf and Ahmed, non-uniformity due to pitting corrosion causes stress concentration at the affected locations along the steel rebars.

$$f_y = \frac{F_{yc}}{A_s} \ (with\ corrosion) < f_y = \frac{F_{yo}}{A_{SO}} \ (no\ corrosion)$$ (28)

The corroded steel reinforcement failed with its average strain, which had a smaller ultimate strain of the uncorroded steel reinforcement. In addition to the steel cross-sectional area and strength reduction, there is a considerable decrease in the ductility of reinforced concrete structures. Furthermore, according to Al-Sakkaf and Ahmed, two methods can be combined to consider the effects of pitting corrosion: the reduction of area and its yield strength. Equation 29 can be used to determine the area reduction, which was originally based on the Stewart model in 2009.[4]

$P(T) = 0.0116\ I_{corr} \times Y \times T$ (mm), (29)

Where:

I_{corr} =   corrosion current density ($\mu A/cm^2$);

T   =   is time (years)

2.2.3   Reduction in Bond Strength

In the proposed model with the surface-based cohesive method, τ_{max}, S_1, and K_{ss} were considered. The maximum bond strength τ_{max} was reduced, which was the value of t_s for cohesive interactions. To reduce the bond strength, τ_{max} and R values of less than 1.0.[4] were used. Equation 30 was used to determine the coefficient reduction of bond strength.

$R = (A_1 + A_2x_p)$ (30)

The reduction is based on the mass loss (x_p) and its areas, which depend on the corrosion current density used in the corrosion acceleration process.[4]

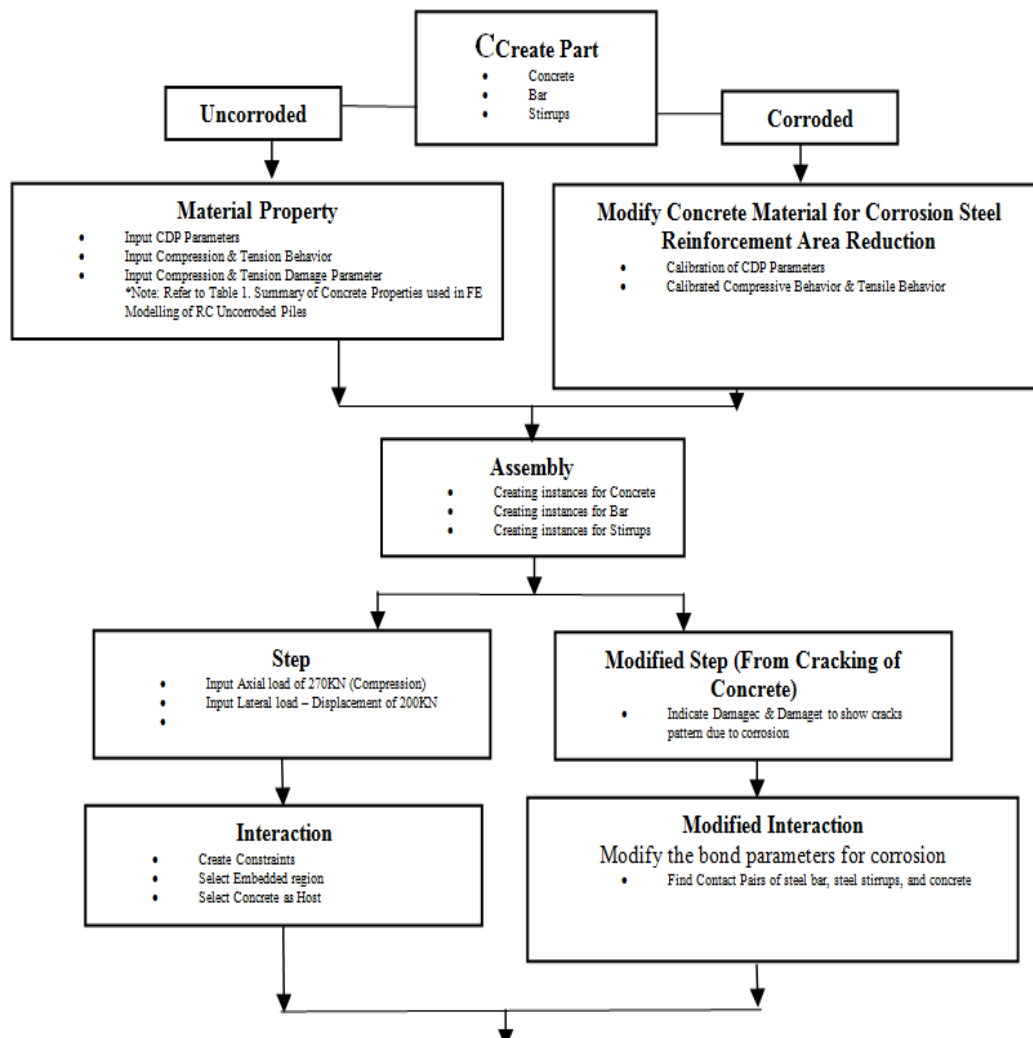### 2.2.3.1   Surface based interaction method

Bond modeling for uncorroded piles assumes perfect bonds between steel and concrete. Different options were used to simulate concrete-steel bonds via finite element analysis using the ABAQUS program. There are two main mechanical approaches that can be used in ABAQUS for surface interactions. The two approaches are surface-based mechanical contact

and surface-based cohesive behavior. The bond behavior is expressed as a linear elastic between traction (t) and separation (δ).[4]

2.2.3.2 Surface-based cohesive behavior

In this method, the bond between two surfaces is linearly elastic between traction (t), bond stress, and separation (δ) a slip.[3] This provides a simplified method for modeling cohesive connections. Surface-based cohesive behavior damage is an interaction property. ABAQUS has two methods of simulating the binding interface behavior using traction(t)-separation (δ) behavior. The two bond-slip behaviors are cohesive elements and surface-based cohesive behavior. Surface-based cohesive behavior is used because of its convenience and effectiveness. The thickness of the interface was considered negligible.[3] The most suitable method for modeling the bond between the steel reinforcement and concrete is the cohesive surface interaction method.[3] Figure 10 illustrates the general procedures for modeling a finite element of uncorroded and corroded reinforced concrete piles.
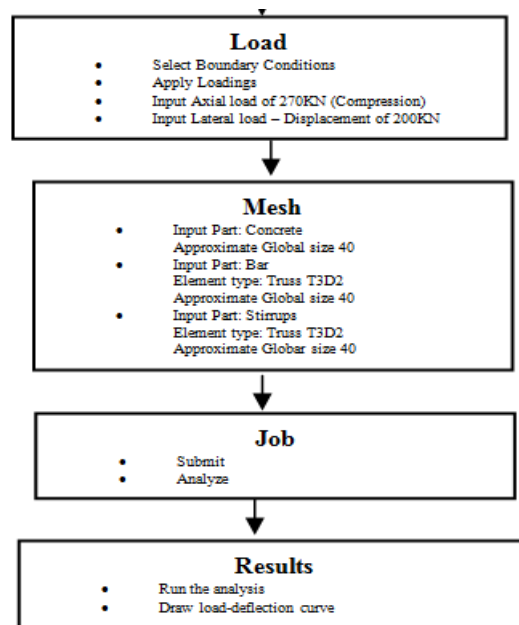
Figure 11: General Procedures for FE of Uncorroded and Corroded Reinforced Concrete Piles.

III. DISCUSSION OF FINITE ELEMENT ANALYSIS RESULTS

To study the effect of corrosion in reinforced concrete piles, finite element FE models were constructed for the same uncorroded and corroded reinforced concrete piles.

3.10   FEA Cracking

In the concrete damaged plasticity CDP model, concrete cracking occurs because of the positive maximum principal plastic strain (PE). The direction of the cracks is normal to the maximum positive principal (PE). Furthermore, with ABAQUS, tensile principal stress can be used, but plastic principal strains provide better visualization of cracks.

Fig. 12 shows the cracking patterns of the concrete obtained from the FEA simulations using ABAQUS. It was observed that in all concentric columns, a significant crack occurred in the upper half portion with rupture on the ligations and concrete core crushing. The FEM cracking patterns were found to be in good agreement with the experimental results.
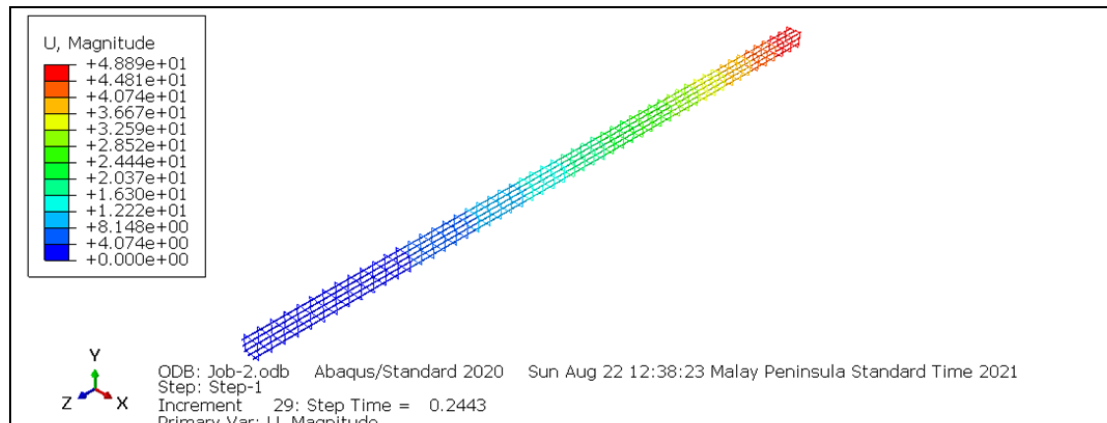
Figure 12: Initiation of cracks.

Corrosion products exerted forces on the concrete surfaces, causing stresses and promoting hairline cracks. Corrosion products continue to expand, which causes further propagation of cracks to the concrete surfaces. Cracks started from the inner surface of the concrete owing to the forces caused by the corrosion products. Figure 12 further illustrates the initiation of cracks beneath the concrete surfaces caused by the expansion of corrosion products as the steel reinforcement disintegrated into the original state, which is also known as the corrosion product.

3.20 Reduction of Mechanical properties of corroded structures

The two main forms of steel reinforcement corrosion are uniform corrosion and pit corrosion. In uniform corrosion, the shape and size of the steel member did not change and were considered to be in a perfect state. Pitting corrosion is common in natural corrosion. There is a local concentration of chloride ions and electrons along the longitudinal reinforcement of the rebar. Uniform corrosion can be simulated by reducing the cross-sectional area of the steel reinforcement. However, it is difficult to model the simulation of the state of pit corrosion because of its randomness along the length of the rebars; thus, the uniform corrosion method of simulation is widely used compared to pit corrosion.

Figure 13: Magnitude of stresses.

Figure 14: Stress along Rebars.

Figure 13 and 14 illustrate the magnitude of the stresses along the reinforced concrete piles. Stresses are higher in the upper middle of the length of piles, as verified from the figures above. At this point, the steel reinforcement experienced a significant deterioration, that is, a reduction in its steel cross-sectional areas. Uniform corrosion existed on the stress point along the length of the rebar at the upper level. Thus, most of the reinforced concrete pile deteriorations lead to spalling of concrete at its point, as shown in Figure 1, wherein a spalling of concrete cover exists and the structures act like without reinforcement.

3.30 Reduction of Bond between Steel and Concrete

The ABAQUS FEM uses nonlinear analysis to simulate the bond-slip behavior of steel reinforcement and concrete. The mechanics calculation formula for the nonlinear element analysis is

$F_i = A_i\,\tau$ (31)

$A_i = 2\pi Rl$ (32)

Where :

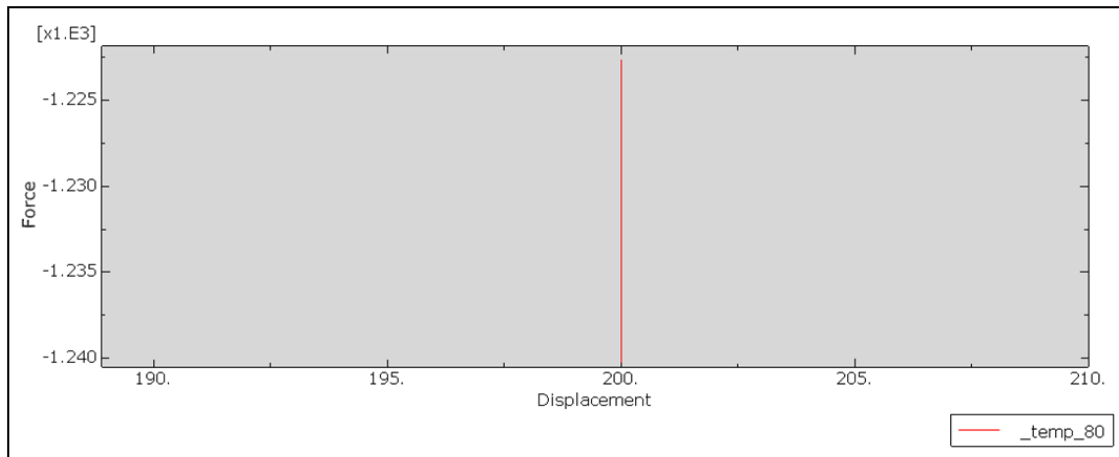| F_i | = | axial force |
A_i	=	interaction area
τ	=	shear stress
R	=	radius of a single rebar at the linkage unit
l	=	spacing of the adjacent spring element

Figure 15: Load-Deflection curve for Corroded Column-Pile.

Figure 15 shows that under severe corrosion conditions, the reduction of bond strength likewise reduces the residual capacity and failure mode of the structural elements. The great displacement of the structures with corroded reinforcement illustrates a significant reduction of the bond between concrete and steel reinforcement. The same also illustrates that it reduces the ductility and bearing capacity of structural members which results into brittle failure.

IV. CONCLUSION

- Constructing a finite element analysis (FEA) model to simulate the effects of corrosion on reinforced concrete piles using ABAQUS is in good agreement with the experimental results and the deterioration of actual reinforced concrete piles.

- The stresses exerted by the corrosion products lead to the initiation of corrosion beneath the concrete surface.

- The loss of bonds between concrete and steel causes sudden failure, and the elements behave as unreinforced columns.

- The spalling of concrete at the upper part requires more anchor reinforcements to avoid early deterioration due to corrosion.

- The crack pattern depends on the bond strength

- If the pile has a sufficient embedded length and the steel reinforcement is well anchored at their ends, a reduction in bond strength does not affect its serviceability and residual life.

V. DECLARATIONS

5.10 Author Contributions

All authors contributed equally to this work, and all authors have read and agreed to the published version of the manuscript.

5.20 Data Availability Statement

The experimental data used to support the findings of this study were included in this study.

5.30 Funding

5.40 Conflict of Interest

The authors declare no conflicts of interest.

5.50 Acknowledgement

VI. REFERENCES

1. Abaqus Analysis User Manual-Abaqus Version, 2012; 6.12.

2. Raza A., Khan Q.Z., Ahmad A., "Numerical Investigation of Load-Carrying Capacity of GFRP-Reinforced Rectangular Concrete Members Using CDP Model in ABAQUS," *Advances in Civil Engineering*, vol. 2019, Article ID 1745341, 2019; 21. https://doi.org/10.1155/2019/1745341.

3. Al-Osta M., Al-Sakkaf H., Sharif, A., Ahmad S., Baluch M., "Finite Element Modeling of Corroded RC beams using Cohesive Surface Bonding Approach." Computers and Concrete, 2018; 22(2): 167-182. DOI: https://doi.org/10.12989/cac.2018.22.2.167.

4. Al-Sakkaf, Hamdi A.,"Modelling of Corroded Reinforced Concrete Beams." King Fahd University of Petroleum Minerals. Dhahran, Saudi Arabia.

5. Jadhav A.M, H.K. Munot H.K., "Analytical Study of Mechanism of Concrete Cracking and Its Propagation due to Corrosion of Reinforcement in RCC." Open Journal of Civil Engineering, 2016; 6: 286-294.

6. Ayinde O.O., Zuo X., Yin G. "Numerical analysis of concrete degradation due to chloride-induced steel corrosion." Advances in Concrete Construction, 2019; 7(4): 203-210. DOI: https://doi.org/10.12989/acc.2019.7.4.203.

7. Bilcik J. and I. Holly.,"Effect of reinforcement corrosion on bond behavior." Procedia Engineering, 2013; 65: 248-253.

8. Chernin L., Val D., "Numerical Modelling of Bond between Concrete and Corroded Reinforcement." School of the Built Environment, Heriot-Watt University, Edinburgh EH14 4AS, UK.

9. Du Qixin., "Finite Element Modelling of Steel / Concrete Bond for Corroded Reinforcement." Univerity of Ottawa, Ottawa, Canada. Department of Civil Engineering.

10. Fernandez I., Herrador M.F., Mari A.R., and Bairan, J.M., "Ultimate capacity of corroded statically indeterminate reinforced concrete members." International Journal of Concrete Structures and Materials, 2018; 2(1).

11. Guifeng Z., Jiankun X., Yaoliang L., Meng Z., "Numerical Analysis of the Degradation Characteristics of Bearing Capacity of a Corroded Reinforced Concrete Beam." *Advances in Civil Engineering*, 2018, Article ID 2492350, 10 pages, 2018. https://doi.org/10.1155/2018/2492350.

12. Hafezolghorani M., Hejazi F., Vaghei R., Jaafar M.S.B., Karimzade K., "Simplified Damage Plasticity Model for Concrete." Structural Engineering International. N.R. 1/2017. DOI: 10.2749/101686616X1081.

13. Hansen E., Saouma V., "Numerical Simulation of Reinforced Concrete Deterioration: Part II-Steel Corrosion and Concrete Cracking." ACI Materials Journal. Technical Paper. Title No. 96-M41

14. Hsuan-The H., and Schnobrich W.C., "Constitutive Modeling of Concrete by Using NonAssociated Plasticity." Journal of Materials in Civil Engineering, 1989; 1(4).

15. Jankowiak T., Lodygowski T., "Indentification of Parameters of Concrete Damage Plasticity Constitutive Model." Foundations of Civil and Environmental Engineering.

16. Jayasinghe J., Mallikarachchi H., Nanayakkara S., and Dias W., "Modelling of Corrosion Induced Cover Cracking in Concrete with Exposed Reinforcement." Moratuwa Engineering Research Conference (MERCon).

17. Li Y.J., Han L.H., Xu W., Tao Z., "Circular concrete-encased concrete-filled steel tube (CFST) stub columns subjected to axial compression." Magazine of Concrete Research, 2016; 68(19): 995-1010. http:dx.doi.org/10.1680/jmacr.15.00359.

18. Khalid N., "Strenght Reduction of Reinforced Concrete Columns subjected to Corrosion Related Cover Spalling". The Graduate Faculty of the University of Akron.

19. Michal S., Andrzej W., "Calibration of the CDP model parameters in Abaqus." The World Congress on Advances in Structural Engineering and Mechanics (ASEM15). Incheon, Korea, 2015; 25-29.

20. Raza A., Khan Q.Z., Ahmad A. "Numerical Invetsigation og Load-Carrying Capacity of GFRP- Reinforced Concrete Members Using CDP Model in ABAQUS". Hindawi Advances in Civil Engineering, Article ID 1745341, 2019; 21. https://doi.org/10.1155/2019/1745341.

21. Roudan B., Kaya A., Adanur S., "Numerical Investigation on the effect of Corrosion on Dynamis Characteristics of Short Piles using ABAQUS Software." International Civil Engineering and Architecture Conference, 2019; 17-20.

22. Sumer Y., and Aktas M., "Defining parameters for concrete damage plasticity model." Challenge Journal of Structural Mechanics, 2015; 1(3): 149-155.

23. Vilnay M., Chernin L., Cotsovos D. "Advanced Material Modelling of Concrete in Abaqus." Conference: 9th International Concrete Conference: Environment, Efficiency and Economic Challenges for Concrete. University of Dundee.